

# A Study of Invisible Neutrino Decay at DUNE and its Effects on $\theta_{23}$ Measurement

Sandhya Choubey,<sup>1,2,3,\*</sup> Srubabati Goswami,<sup>4,†</sup> and Dipyaman Pramanik<sup>1,3,‡</sup>

<sup>1</sup>*Harish-Chandra Research Institute,*

*Chhatnag Road, Jhansi, Allahabad 211 019, India*

<sup>2</sup>*Department of Physics, School of Engineering Sciences,*

*KTH Royal Institute of Technology,*

*AlbaNova University Center, 106 91 Stockholm, Sweden*

<sup>3</sup>*Homi Bhabha National Institute, Training School Complex,*

*Anushakti Nagar, Mumbai 400085, India*

<sup>4</sup>*Physical Research Laboratory, Navrangpura, Ahmedabad 380 009, India*

## Abstract

We study the consequences of invisible decay of neutrinos in the context of the DUNE experiment. We assume that the third mass eigenstate is unstable and decays to a light sterile neutrino and a scalar or a pseudo-scalar. We consider DUNE running in 5 years neutrino and 5 years antineutrino mode and a detector volume of 40 kt. We obtain the bounds on the rest frame life time  $\tau_3$  normalized to the mass  $m_3$  as  $\tau_3/m_3 > 4.50 \times 10^{-11}$  s/eV at 90% C.L. for a normal hierarchical mass spectrum. We also find that DUNE can discover neutrino decay for  $\tau_3/m_3 > 4.27 \times 10^{-11}$  s/eV at 90% C.L. In addition, for an unstable  $\nu_3$  with an illustrative value of  $\tau_3/m_3 = 1.2 \times 10^{-11}$  s/eV, the no decay case gets disfavoured at the  $3\sigma$  C.L. At 90% C.L. the allowed range for this true value is obtained as  $1.71 \times 10^{-11} > \tau_3/m_3 > 9.29 \times 10^{-12}$  in units of s/eV. We also study the correlation between a non-zero  $\tau_3/m_3$  and standard oscillation parameters and find an interesting correlation in the appearance channel probability with the mixing angle  $\theta_{23}$ . This alters the octant sensitivity of DUNE, favorably (unfavorably) for true  $\theta_{23}$  in the lower (higher) octant. The effect of a decaying neutrino does not alter the hierarchy or CP discovery sensitivity of DUNE in a discernible way.

---

\*Electronic address: sandhya@hri.res.in

†Electronic address: sruba@prl.res.in

‡Electronic address: dipyamanpramanik@hri.res.in

## I. INTRODUCTION

Neutrino oscillation experiments have established that neutrinos are massive and there is mixing among all the three flavors. The neutrino oscillation parameters – namely the two mass squared differences  $\Delta m_{21}^2 = m_2^2 - m_1^2$  and  $|\Delta m_{31}^2| = |m_3^2 - m_1^2|$ ,  $m_1, m_2, m_3$  being the mass states and the three mixing angles  $\theta_{12}, \theta_{13}$  and  $\theta_{23}$  have been determined with considerable precision by global oscillation analysis of world neutrino data [1, 2]. The unknown oscillation parameters are: (i) the neutrino mass hierarchy i.e whether  $m_3 > m_2 > m_1$  leading to normal hierarchy (NH) or if  $m_3 < m_2 \approx m_1$  resulting in inverted hierarchy (IH); (ii) the octant of  $\theta_{23}$  – if  $\theta_{23} < 45^\circ$  it is said to be in the lower octant (LO) and if  $\theta_{23} > 45^\circ$  it is in the higher octant (HO); (iii) the CP phase  $\delta_{CP}$ . There are some indications of these quantities from the recent results of the ongoing experiments T2K [3] and NO $\nu$ A [4, 5]. However no clear conclusions have been reached yet. While more statistics from these experiments will be able to give some more definite ideas regarding the three unknowns, the precision determination is expected to come from the Fermilab based broadband experiment DUNE which has a baseline of 1300 km. With a higher baseline than T2K and NO $\nu$ A, DUNE is more sensitive to the Earth matter effect which gives it an edge to determine the mass hierarchy and octant and hence  $\delta_{CP}$  by resolving the wrong-hierarchy/wrong-CP or wrong-octant/wrong-CP solutions. Thus, it is expected that DUNE will be able to determine the above three outstanding parameters with considerable precision with its projected run. For a recent analysis, in view of the latest NO $\nu$ A results see [6].

This capability of DUNE, to make precision measurements also makes it an ideal experiment to test sub-dominant new physics effects. One of the widely studied subdominant effect, in the context of neutrino experiments, is the "invisible decay" of neutrinos i.e decay to sterile states. This can arise if neutrinos are: (i) Dirac particles and there is a coupling between the neutrinos and a light scalar boson [7, 8]. This allows the decay  $\nu_j \rightarrow \bar{\nu}_{iR} + \chi$  where  $\bar{\nu}_{iR}$  is a right-handed singlet and  $\chi$  is an iso-singlet scalar carrying a lepton number. (ii) Majorana particles with a pseudo-scalar coupling with a Majoron [9, 10] and a sterile neutrino giving rise to the decay  $\nu_j \rightarrow \nu_s + J$ . The Majoron should be dominantly singlet to comply with the constraints from LEP data on the Z decay to invisible particles. Such models have been discussed in [11]. In both the cases all the final state particles are sterile and invisible. The other possibility of "visible decay" occurs if neutrinos decay to active

neutrinos [12–14]. The decay modes are  $\nu_j \rightarrow \bar{\nu}_i + J$  or  $\nu_j \rightarrow \nu_i + J$ . For Majorana neutrinos both  $\bar{\nu}_i$  ( $\nu_i$ ) can interact as a flavor state  $\bar{\nu}_\alpha$  ( $\nu_\alpha$ ) according to  $U_{\alpha i}^2$  and thus the decay product can be observed in the detector. For recent studies on implications of visible decay for long baseline experiments see [15, 16].

Neutrino decay manifests itself through a term of the form  $\exp(-\frac{m_i L}{\tau_i E})$  which gives the fraction of neutrinos of energy  $E$  that decays after travelling through a distance  $L$ . Here,  $\tau_i$  denotes the rest frame life time of the state with mass  $m_i$ .

Neutrino decay as a solution to explain the depletion of the solar neutrinos has been considered very early [17]. Subsequently, many authors have studied the neutrino oscillation plus decay solution to the solar neutrino problem and put bounds on the lifetime of the unstable state [8, 18–24]. These studies considered  $m_2$  to be the unstable state and obtained bounds on  $\tau_2$ . This is plausible, since,  $U_{e3}$  being relatively small, the admixture of  $\nu_3$  state in the solar  $\nu_e$  can be taken to be small. Note that most of these studies have been performed prior to the discovery of non-zero  $\theta_{13}$ . Typical bounds obtained from solar neutrino data is  $\tau_2/m_2 > 8.5 \times 10^{-7}$  s/eV [23]. A recent study performed in ref. [25] has obtained bound on both  $\tau_2$  and  $\tau_1$  including low energy solar neutrino data. Bound on  $\tau_2$  or  $\tau_1$  can also come from supernova neutrinos. The bound obtained in ref. [26] is  $\tau/m > 10^5$  s/eV from SN1987A data.

Bounds on the  $\nu_3$  lifetime have been obtained in the context of atmospheric and long-baseline (LBL) neutrinos. A pure neutrino decay solution (without including neutrino mixing into account) to the atmospheric neutrino problem was discussed in [27] and it was shown that this solution gives a poor fit to the data. Neutrino decay with non-zero neutrino mixing angle was first considered in [28, 29] where it was assumed that the state  $\nu_\mu$  has an unstable component. It was shown that the neutrino decay with mixing can reproduce the L/E distribution of the SuperKamiokande(SK) data. Later this scenario was reanalyzed in [30] using the zenith angle dependence of the SK data rather than the L/E distribution and it was shown that this gives a poor fit to the SK data. In [28] and [30] the  $\Delta m^2$  dependent terms were averaged out since it was assumed that  $\Delta m^2 > 0.1$  eV<sup>2</sup> to comply with the constraints coming from K decays [28]. However, these constraints can be evaded if the unstable state decays to some state with which it does not mix. Two scenarios have been considered in the literature in this context. The first analysis was done in ref. [31], where  $\Delta m^2$  was kept unconstrained and it explicitly appeared in the probabilities. It was shown

that if one fits SK data with this scenario then the best-fit comes with a non-zero value of the decay parameter and  $\Delta m^2 \sim 0.003 \text{ eV}^2$ , implying that oscillation combined with small decay can give a better fit to the data. Later in ref. [32] the possibility that  $\Delta m^2 \ll 10^{-4} \text{ eV}^2$  was considered. In this case also the probability does not contain  $\Delta m^2$  explicitly and the scenario correspond to decay plus mixing. In [32] it was shown that this scenario can give a good fit to the SK data but subsequent analysis by the SK collaboration revealed that the decay plus mixing scenario of [32] gives a poorer fit to data than only oscillation [33]. A global analysis of atmospheric and long-baseline neutrino data in the framework of the oscillation plus decay scenario considered in [31] was done in [34]. Although only oscillation gave the best- fit to the SK data, a reasonable fit was also obtained with oscillation plus decay. However, with the addition of the data from the LBL experiment MINOS, the quality of the fit became poorer. They put a bound on  $\tau_3/m_3 \geq 2.9 \times 10^{-10} \text{ s/eV}$  at the 90% C.L. Subsequently, analysis of oscillation plus decay scenario with unconstrained  $\Delta m^2$  have been performed in [35] in the context of MINOS and T2K data and the bound  $\tau_3/m_3 > 2.8 \times 10^{-12} \text{ s/eV}$  at 90% C.L. was obtained. Most of the above analyses have been performed in the two generation limit and matter effect in presence of decay, in the context of atmospheric and LBL neutrinos have not been studied. Expected constraint on  $\tau_3/m_3 > 7.5 \times 10^{-11} \text{ s/eV}$  (95% C.L.) in the context of the medium baseline reactor neutrino experiment like JUNO has been obtained in ref. [36] using a full three generation picture in vacuum.

Decay of ultrahigh energy astrophysical neutrinos have been considered by many authors [37–40]. A recent study performed in ref. [41] states that the IceCube experiment can reach a sensitivity of  $\tau/m \geq 10 \text{ s/eV}$  for both hierarchies for 100 TeV neutrinos coming from a source at a distance of 1 Gpc.

In this paper we study the constraints on  $\tau_3/m_3$  from simulated data of the DUNE experiment assuming invisible decay of the neutrinos. We perform a full three flavor study and include the matter effect during the propagation of the neutrinos through the Earth. We obtain constraints on the life time of the unstable state from the simulated DUNE data. For obtaining this we assume the state  $\nu_3$  to be unstable and obtain the constraints on  $\tau_3/m_3$ . We also study the discovery potential and precision of measuring  $\tau_3/m_3$  at DUNE assuming decay is present in nature. In addition, we explore how the decay lifetime  $\tau_3$  is correlated with the mixing angle  $\theta_{23}$  leading to approximate degeneracy between the two parameters. We will study how this affects the sensitivity of DUNE to the mixing angle  $\theta_{23}$

and its octant. The sensitivity of DUNE, to determine the standard oscillation parameters like the mass hierarchy and  $\delta_{CP}$  could also in principle get affected if the heaviest state is unstable, and we study this here.

The plan of the paper is as follows. In the next section we discuss the propagation of neutrinos through Earth matter when one of the state undergoes decay to invisible states. Section III contains the experimental and simulation details. The results are presented in the section IV and finally we conclude in section V.

## II. NEUTRINO PROPAGATION IN PRESENCE OF DECAY

Assuming the  $\nu_3$  state to decay into a sterile neutrino and a singlet scalar ( $\nu_3 \rightarrow \bar{\nu}_4 + J$ ), the flavor and mass eigenstates get related as,

$$\begin{pmatrix} \nu_\alpha \\ \nu_s \end{pmatrix} = \begin{pmatrix} U & 0 \\ 0 & 1 \end{pmatrix} \begin{pmatrix} \nu_i \\ \nu_4 \end{pmatrix}. \quad (1)$$

Here,  $\nu_\alpha$  with  $\alpha = e, \mu, \tau$  denote the flavor states and  $\nu_i$ ,  $i = 1, 2, 3$  denote the three mass states corresponding to the active neutrinos.  $U$  is the standard  $3 \times 3$  PMNS mixing matrix. We assume that  $m_3 > m_2 > m_1 > m_4$  for NH while  $m_2 \approx m_1 > m_3 > m_4$  for IH. This implies that for both NH and IH the third mass state can decay to a lighter sterile state. Note that  $\Delta m_{34}^2$  is unconstrained from meson decay bound since  $m_4$  is the mass of a sterile state with which the active neutrinos do not mix. The effect of decay can be incorporated in the propagation equation by introducing a term  $m_3/\tau_3$  in the evolution equation:<sup>1</sup>

$$i \frac{d}{dx} \begin{pmatrix} \nu_e \\ \nu_\mu \\ \nu_\tau \end{pmatrix} = \left[ U \left[ \frac{1}{2E} \begin{pmatrix} 0 & 0 & 0 \\ 0 & \Delta m_{21}^2 & 0 \\ 0 & 0 & \Delta m_{31}^2 \end{pmatrix} - i \frac{m_3}{2E\tau_3} \begin{pmatrix} 0 & 0 & 0 \\ 0 & 0 & 0 \\ 0 & 0 & 1 \end{pmatrix} \right] U^\dagger + \begin{pmatrix} A & 0 & 0 \\ 0 & 0 & 0 \\ 0 & 0 & 0 \end{pmatrix} \right] \begin{pmatrix} \nu_e \\ \nu_\mu \\ \nu_\tau \end{pmatrix}, \quad (2)$$

where the term  $A = 2\sqrt{2}G_F n_e E$  represents the matter potential due to neutrino electron scattering in matter,  $G_F$  denotes the Fermi coupling,  $E$  is the energy, and  $n_e$  the electron density. For the antineutrinos the matter potential comes with a negative sign. The fourth sterile state being decoupled from the other states except through the interaction which

---

<sup>1</sup> This implicitly assume that the neutrino mass matrix and the decay matrix can be simultaneously diagonalised and the mass eigenstates are the same as the decay eigenstates [26, 42]

induces the decay, does not affect the propagation. We solve the Eq. (2), in matter numerically using Runge-Kutta technique assuming the PREM density profile [43] for the Earth matter. In section IV we will show the plots of the appearance channel probability  $P_{\mu e}$  and disappearance channel probability  $P_{\mu\mu}$  as a function of neutrino energy.

### III. EXPERIMENT AND SIMULATION DETAILS

DUNE (Deep Underground Neutrino Experiment) is a long baseline neutrino oscillation experiment proposed to be built in USA. DUNE will consist of a neutrino beam from Fermilab to Sanford Underground Research Facility [44–47]. The source of the beam will consist of a 80-120 GeV proton beam which will give the neutrino beam eventually. There will be a 34-40 kt liquid Argon time projection chamber (LArTPC) at the end of the beam, at 1300 km from the source. We use the GLoBES package [48, 49] to simulate the DUNE experiment. In our simulation, we have used neutrino and antineutrino flux from a 120 GeV, 1.2 MW proton beam at Fermilab and a 40 kt far detector. All our simulations are for a runtime of 5+5 years (5 years in  $\nu$  and 5 years in  $\bar{\nu}$ ) and we take both appearance and disappearance channels into account, unless otherwise stated. For the charged current (CC) events we have used 20% energy resolution for the  $\mu$  and 15% energy resolution for the  $e$ .

The primary background to the electron appearance and muon disappearance signal events come from the neutral current (NC) background and the intrinsic  $\nu_e$  contamination in the flux. In addition, there is a wrong-sign component in the flux. The problem of wrong-sign events is severe for the antineutrino run, since the neutrino component in the antineutrino flux is larger than the antineutrino component in the neutrino flux. We have taken all these backgrounds into account in our analyses. In order to reduce the backgrounds, several cuts are taken. The effects of these cuts have been imposed in our simulation through efficiency factor of the signal. We have included 2% (10%) signal (background) normalization errors and 5% energy calibration error as systematic uncertainties. The full detector specification can be found in Ref. [45] and we have closely followed it.

Throughout this paper we use the following true values for the standard oscillation parameters:  $\theta_{12} = 34.8^\circ$ ,  $\theta_{13} = 8.5^\circ$ ,  $\theta_{23} = 42.0^\circ$  for lower octant and  $\theta_{23} = 48.0^\circ$  for higher octant,  $\Delta m_{21}^2 = 7.5 \times 10^{-5}$  eV,  $\Delta m_{31}^2 = 2.457 \times 10^{-3}$  eV and  $\delta_{CP} = -90^\circ$ . We marginalize our  $\chi^2$  over standard oscillation parameters. We keep the hierarchy normal in the simulated

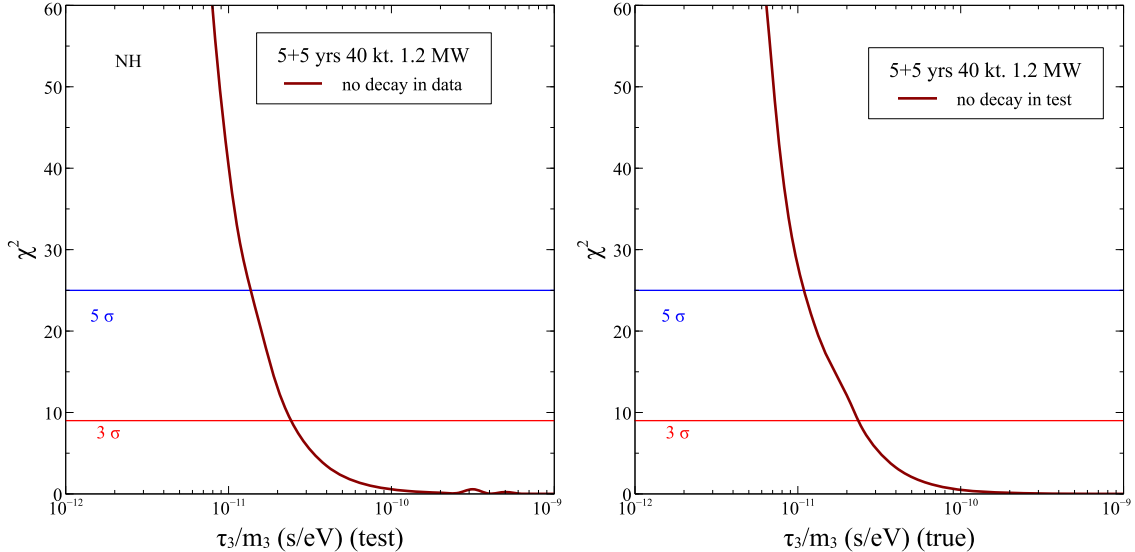


FIG. 1: The left-panel of this figure shows the expected sensitivity of DUNE to constraining the decay parameter  $\tau_3/m_3$ . The right-panel of this figure presents the potential of DUNE to discover a decaying  $\nu_3$ . See text for details.

data for all the results presented in this paper.

#### IV. RESULTS

We will first present results on how well DUNE will be able to constrain or discover the lifetime of the unstable  $\nu_3$  state. We will then turn our focus on how the measurement of standard oscillation physics at DUNE might get affected if  $\nu_3$  were to be unstable.

##### A. Constraining the $\nu_3$ lifetime

The left-panel of Fig. 1 shows the potential of DUNE to constrain the lifetime of  $\nu_3$  normalized to its mass  $m_3$ . In order to obtain this curve we generate the data for a no-decay case and fit this data for an unstable  $\nu_3$ . We marginalize the  $\chi^2$  over all standard oscillation parameters as mentioned above. We see that at the  $3\sigma$  level DUNE could constrain  $\tau_3/m_3 > 2.38 \times 10^{-11}$  s/eV, whereas at 90% C.L. the corresponding expected limit would be  $\tau_3/m_3 > 4.50 \times 10^{-11}$  s/eV. This can be compared with the current limit on  $\tau_3/m_3 > 2.8 \times 10^{-12}$  s/eV that we have from combined MINOS and T2K analysis [35]. Therefore, DUNE is expected

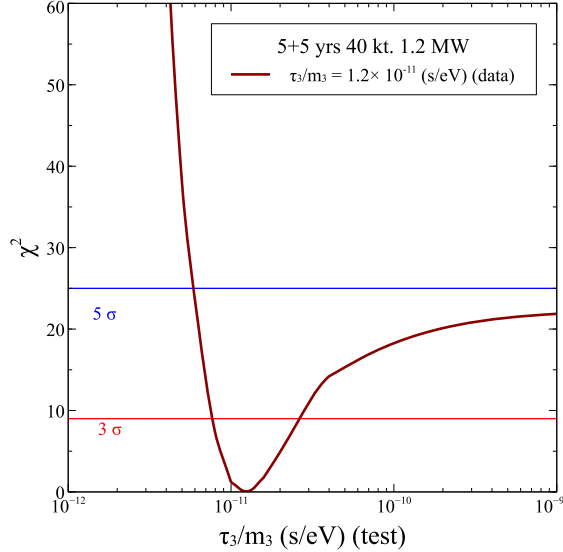


FIG. 2:  $\chi^2$  projections as a function of  $\tau_3/m_3$  (true).

to improve the bounds on  $\nu_3$  lifetime by at least one order of magnitude. The right-panel of Fig. 1 shows the discovery potential of a decaying neutrino at DUNE. To obtain this curve we generated the data taking a decaying  $\nu_3$  into account and fitted it with a theory for stable neutrinos. The  $\chi^2$  so obtained is then marginalized over the standard oscillation parameters in the fit. The resultant marginalized  $\chi^2$  is shown in the right-panel of Fig. 1 as a function of the  $\tau_3/m_3$ (true). DUNE is expected to discover a decaying neutrino at the  $3\sigma$  C.L. for  $\tau_3/m_3 > 2.38 \times 10^{-11}$  s/eV and the 90% C.L. for  $\tau_3/m_3 > 4.27 \times 10^{-11}$  s/eV.

Assuming that the  $\nu_3$  is indeed unstable with a decay width corresponding to  $\tau_3/m_3 = 1.2 \times 10^{-11}$  s/eV, we show in Fig. 2 how well DUNE will be able to constrain the lifetime of the decaying  $\nu_3$ . It is seen from the figure that in this case not only can DUNE exclude the no decay case above  $3\sigma$ , but can also measure the value of the decay parameter with good precision. The corresponding  $3\sigma$  and 90% C.L. ranges are  $2.63 \times 10^{-11} > \tau_3/m_3 > 7.62 \times 10^{-12}$  and  $1.71 \times 10^{-11} > \tau_3/m_3 > 9.29 \times 10^{-12}$  in units of s/eV, respectively.

## B. Constraining $\theta_{23}$ and its Octant

Fig. 3 gives the neutrino oscillation probability for both the appearance and disappearance channels. The left-panels give the probability for the appearance channel while the right-panels show the probability for the disappearance channel. The top-panels show the impact

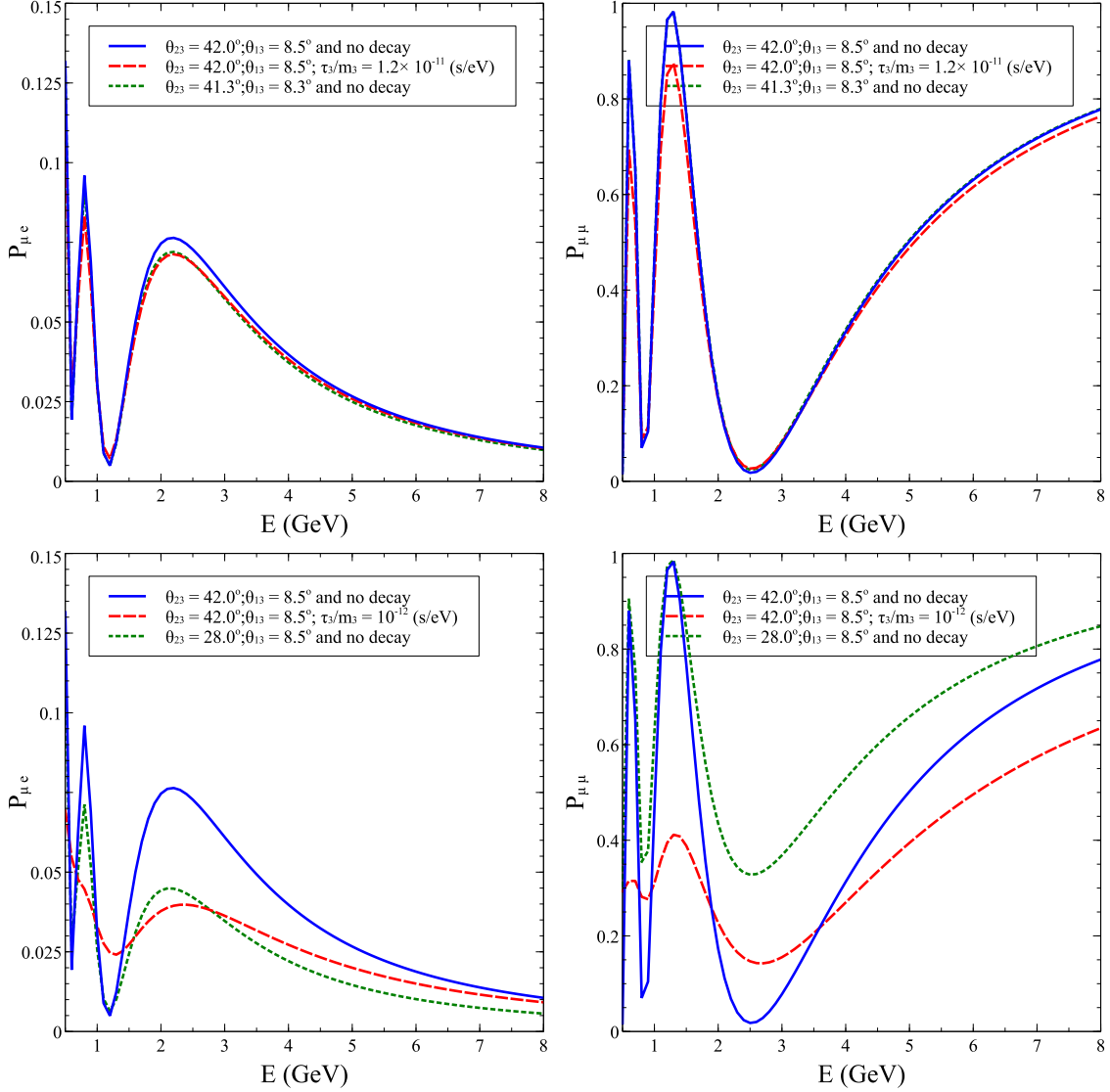


FIG. 3: The appearance (left-panels) and disappearance (right-panels) channel neutrino probabilities as a function of neutrino energy. The different lines are described in the legends and also in the text. The top panels show the effect of  $\nu_3$  decay for a larger value of  $\tau_3/m_3$  while the bottom panels show the effect for a smaller value of  $\tau_3/m_3$ .

of decay on the probabilities for  $\tau_3/m_3 = 1.2 \times 10^{-11}$  s/eV while the bottom-panels show the effect when  $\tau_3/m_3 = 1.0 \times 10^{-12}$  s/eV. The solid lines and the short-dashed lines show the probabilities for the standard stable case. The blue solid lines in all the four panels are for  $\theta_{23} = 42^\circ$  and  $\theta_{13} = 8.5^\circ$  and no decay. The change in the probabilities when decay is switched on for the same set of oscillation parameters is shown in all the panels

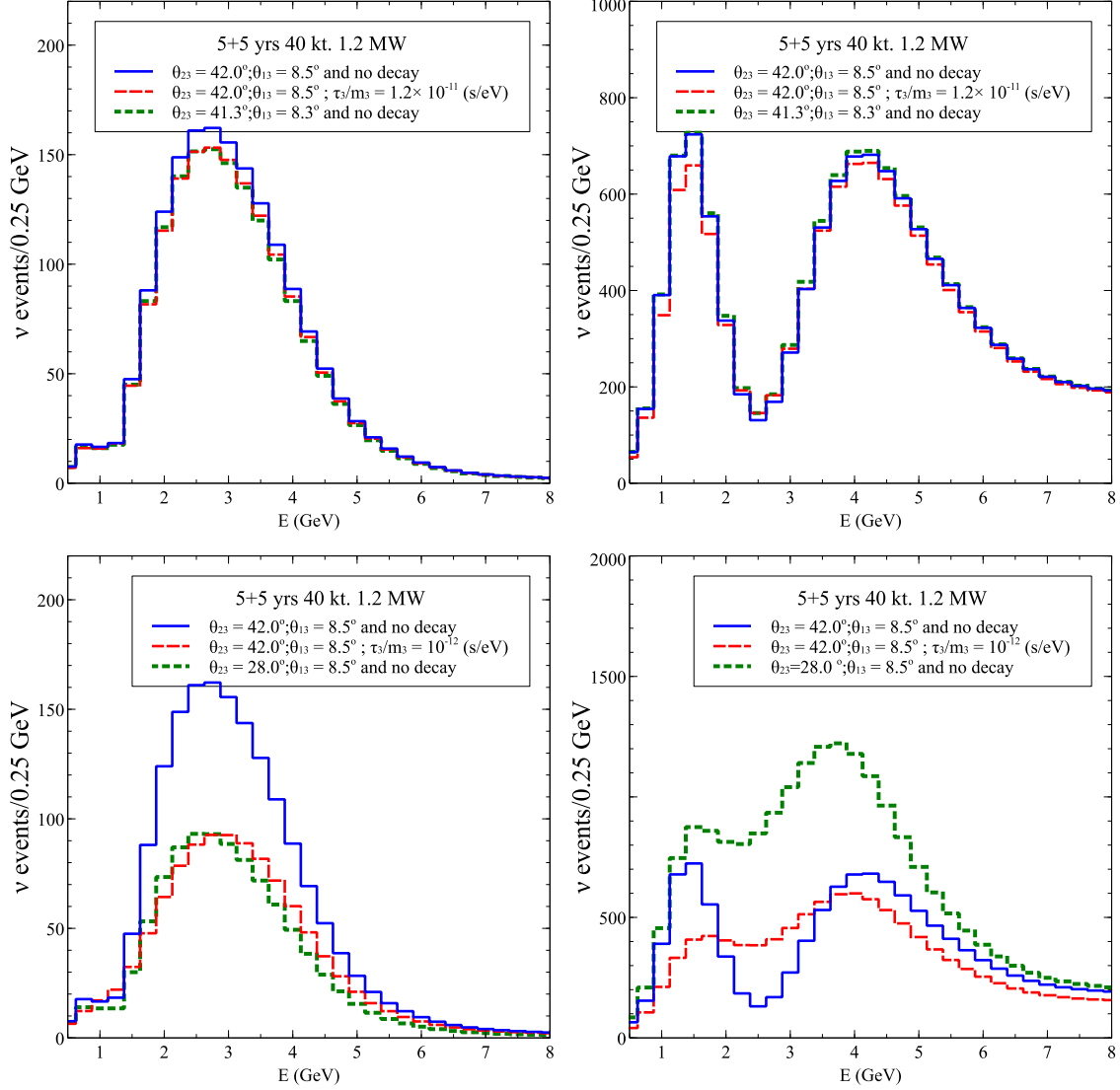


FIG. 4: Same as in Fig. 3 but showing neutrino events at DUNE instead of probabilities. The left-panels show the electron appearance events, while the right-panels show the muon disappearance events. The top panels shows the impact of a larger  $\tau_3/m_3$ , while the bottom panels are for a smaller  $\tau_3/m_3$ .

by the red long-dashed line. The first thing to note from this figure is that  $P_{\mu e}$  decreases while  $P_{\mu\mu}$  increases at the oscillation maximum. The opposite trend is seen for the case when the oscillatory term goes to zero. However, net probability for both appearance as well as disappearance channels decrease in the case of decay. This is because in our model the  $\nu_3$  decays to invisible states which do not show-up at the detector. As expected, the

extent of decrease of the probability increases as we lower  $\tau_3/m_3$  or in other words increase the decay rate, as can be seen by comparing the top panels with the bottom ones. For  $\tau_3/m_3 = 1.0 \times 10^{-12}$  s/eV we see a drastic change in the probability plots, thereby allowing DUNE to restrict these values of  $\tau_3/m_3$ , as we had seen in the previous section.

Next we turn to show the correlation between the decay lifetime  $\tau_3/m_3$  and the mixing angles, in particular, the mixing angle  $\theta_{23}$ . In Fig. 3 we show that the appearance channel probability  $P_{\mu e}$  for the case with decay (shown by the red long-dashed lines) can be mimicked to a large extent by the no decay scenario if we reduce the value of  $\theta_{23}$ . These probability curves are shown by the green short-dashed lines. For the top-panels we can achieve reasonable matching between the decay and no decay scenario if the  $\theta_{23}$  is reduced from  $42^\circ$  to  $41.3^\circ$ . In the lower panels, since the  $\nu_3$  lifetime is chosen to be significantly smaller, we see a more drastic effect of  $\theta_{23}$  on  $P_{\mu e}$ . In the lower panels the with decay case for  $\theta_{23} = 42^\circ$  can be matched by the no decay case if we take a much reduced  $\theta_{23} = 28^\circ$ . In all cases, the disappearance channel is never matched between the red long-dashed and green short-dashed lines. This implies that while the appearance channel is expected to see degenerate solutions in  $\theta_{23}$  due to decay, the disappearance channel would not. Hence, the disappearance channel would always work towards breaking this degeneracy.

This correlation between  $\tau_3/m_3$  and  $\theta_{23}$  in  $P_{\mu e}$  can be understood as follows. No decay corresponds to infinite  $\tau_3/m_3$ . As we reduce  $\tau_3/m_3$ ,  $\nu_3$  starts to decay into invisible states reducing the net  $P_{\mu e}$ . This reduction increases as we continue to lower  $\tau_3/m_3$ . On the other hand, it is well known that  $P_{\mu e}$  increases linearly with  $\sin^2 \theta_{23}$  at leading order. Therefore, it is possible to obtain a given value of  $P_{\mu e}$  either by reducing  $\tau_3/m_3$  or by reducing  $\sin^2 \theta_{23}$  for no decay. Likewise, it will be possible to compensate the decrease in  $P_{\mu e}$  due to decay by increasing the value of  $\sin^2 \theta_{23}$ . The survival channel on the other hand, depends inversely on  $\sin^2 2\theta_{23}$  at leading order. Hence, a reduction of  $\theta_{23}$  increases  $P_{\mu\mu}$  at the maximum of oscillations when the oscillatory term goes to 1. For the energies for which the latter is zero, the value of  $\sin^2 2\theta_{23}$  is inconsequential. Since decay causes  $P_{\mu\mu}$  to decrease when the oscillatory is zero and increase when it is one, it is impossible to match a disappearance spectrum corresponding to decay with one where neutrinos are taken as stable and with a different  $\theta_{23}$ .

In order to see the correlation between  $\tau_3/m_3$  and  $\theta_{23}$  at the event level, we plot in Fig. 4 the appearance (electron) and disappearance (muon) events for 5 years of running of DUNE

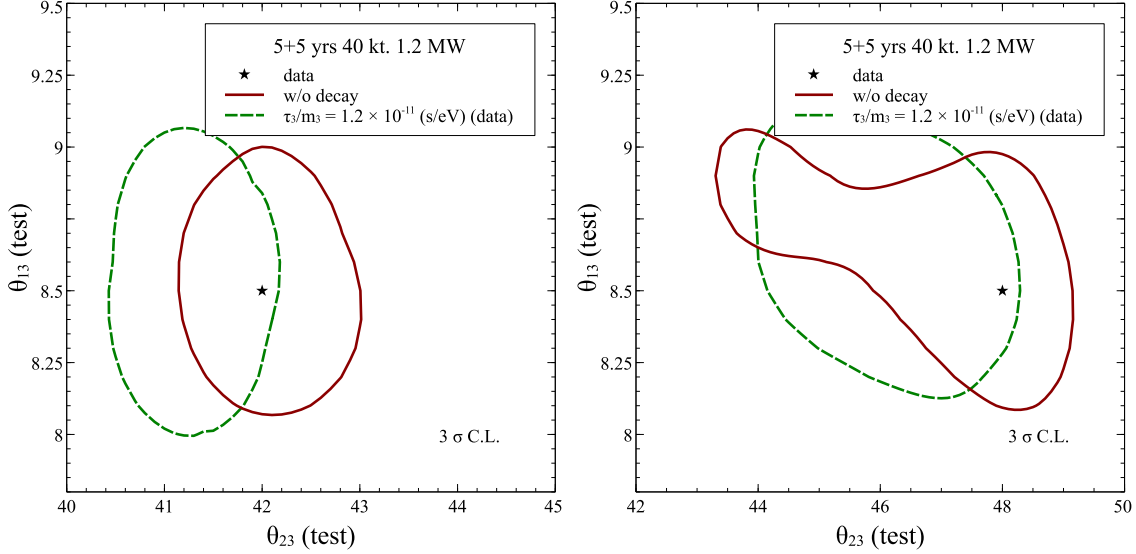


FIG. 5: The plots show the expected  $3\sigma$  C.L. contours in the  $\theta_{23} - \theta_{13}$  plane for the case when the data is simulated in the lower octant  $\theta_{23} = 42^\circ$  (left-panel) and in the higher octant  $\theta_{23} = 48^\circ$  (right-panel). The black stars show the data points in the plane. The dark red solid curves show the expected  $3\sigma$  contour for the standard scenario in absence of decay in data and theory. The green dashed curves show the  $3\sigma$  contour for the case when the data corresponds to a decaying  $\nu_3$  with  $\tau_3/m_3 = 1.2 \times 10^{-11}$  s/eV, which is fitted with a theory where all neutrinos are taken as stable.

in the neutrino channel. One will expect a similar behaviour for the antineutrinos as well. The respective panels and the three plots in each panel are arranged in exactly the same way as in Fig. 3. We note that all the features that were visible at the probability level in Fig. 3 is also seen clearly at the events level in Fig. 4. Neutrino events are seen to reduce with the onset of neutrino decay, with the extent of reduction increasing sharply with the value of the decay rate ( $1/\tau_3$ ). The electron event spectrum for the case with decay can be seen to be roughly mimicked with that without decay but with a lower value of the  $\theta_{23}$ , the required change in the value of  $\theta_{23}$  increasing with the decay rate ( $1/\tau_3$ ). The muon spectrum on the other hand, does not show this behaviour and is hence expected to be instrumental in breaking the approximate degeneracy between  $\tau_3/m_3$  and  $\theta_{23}$ .

The impact of decay on the expected constraints on  $\theta_{23}$  (and  $\theta_{13}$ ) is shown in Fig. 5. The left panel shows the results when the data is generated at  $\theta_{23}$  belonging to lower octant,

while the right panel gives the results for data corresponding to  $\theta_{23}$  in the higher octant. The point where the data is generated is marked by a star in the  $\theta_{23} - \theta_{13}$  plane. The expected contours correspond to  $3\sigma$  C.L. The dark red solid lines are obtained for the standard case when neutrinos are taken as stable in both the data as well as the fit. The green dashed ones are obtained when we simulate the data assuming an unstable  $\nu_3$  with  $\tau_3/m_3 = 1.2 \times 10^{-11}$  s/eV, but fit it with the standard case assuming stable neutrinos. The contours are marginalized over all oscillation parameters. The impact of decay is visible in both panels. Though the contours change in both mixing angles, the impact on  $\theta_{23}$  is seen to be higher than the impact on  $\theta_{13}$ . The green contours are shifted to lower values of  $\theta_{23}$  in both panels. The reason for this was discussed earlier through Figs. 3 and 4. The electron appearance data corresponding to a decaying  $\nu_3$  can be fitted with a theory for stable neutrinos by shifting  $\theta_{23}$  to lower values in the fit. We had also noted that for the muon disappearance events such an approximate degenerate solution did not exist. However, since the appearance data dominates the fit over the disappearance data, it manifests in the shifting of the expected contours to lower  $\theta_{23}$  values, with the true value of  $\theta_{23}$  barely allowed at the  $3\sigma$  C.L. We also note that since the general trend is to shift the fitted  $\theta_{23}$  to lower values, for the case where the data corresponds to the higher octant (right-panel), DUNE could face additional challenges for  $\theta_{23}$  octant discrimination.

In order to study the impact of decay on the expected  $\theta_{23}$  octant sensitivity of DUNE, we first show in Fig. 6 the  $\chi^2$  as a function of  $\theta_{23}(\text{test})$ . The left (right) panel is for the case when the data is generated at  $\theta_{23} = 42^\circ(48)^\circ$ . The dark red solid curve shows the standard case of stable neutrinos. The curve in the left-panel shows that the wrong octant ( $\theta_{23} > 45^\circ$ ) for this case would be disfavored at slightly below  $5\sigma$ . The effect of decay is shown via the green dashed curve, wherein we generate the data again at  $\theta_{23} = 42^\circ$  but now for unstable  $\nu_3$  with  $\tau_3/m_3 = 1.2 \times 10^{-11}$  s/eV. We fit this data with a theory with stable neutrinos and the corresponding  $\chi^2$  is marginalized over all other oscillation parameters. We see that the green dashed curve is shifted with respect to the dark red solid curve. We also note that the octant sensitivity appears to have increased since the lowest  $\chi^2$  in the wrong octant for this case corresponds to greater than  $5\sigma$ . The right-panel is also similar except that for this case the data for both dark red solid and green dashed lines are generated at the higher octant value  $\theta_{23} = 48^\circ$ . We note that even for the standard stable case, the wrong octant ( $\theta_{23} < 45^\circ$ ) for this case would be disfavored at only the  $3\sigma$  C.L. With the inclusion of decay

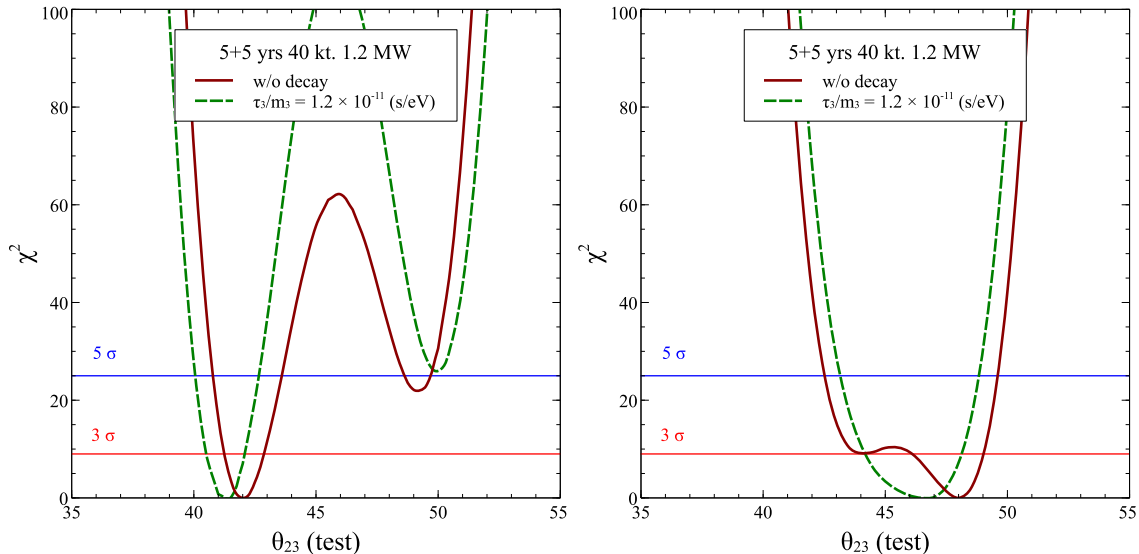


FIG. 6:  $\chi^2$  as a function of  $\theta_{23}(\text{test})$ . The left (right) panel is for the case when the data is generated at  $\theta_{23} = 42^\circ(48)^\circ$ . The dark red solid curve is for the standard case while the green dashed curve is for the case when the data is generated for unstable  $\nu_3$  with  $\tau_3/m_3 = 1.2 \times 10^{-11}$  s/eV but it is fitted assuming stable neutrinos.

in the data, the fitted  $\theta_{23}$  is shifted in this case is such a way that even the best-fit  $\theta_{23}$  in the wrong octant goes to lower values and very low values of  $\chi^2$  can be found in the wrong octant ( $\theta_{23} < 45^\circ$ ). We will see the impact of this on the octant sensitivity of DUNE next.

The Fig. 7 shows the octant sensitivity for 5+5 years of  $(\nu + \bar{\nu})$  running of DUNE. The dark-red solid curve shows the octant sensitivity for the standard case with stable neutrinos. The green dashed curve is for the case when  $\nu_3$  is taken as unstable with  $\tau_3/m_3 = 1.2 \times 10^{-11}$  s/eV in the data, but in the fit we keep it to be stable. We note that the octant sensitivity of DUNE improves for the green dashed line in the lower octant, but in the higher octant it deteriorates. This is consistent with our observations in Fig. 6.

### C. CP-violation and Mass Hierarchy Sensitivity

In Fig. 8 we show the expected CP-violation sensitivity at DUNE. As before, the dark red solid curve is for standard case of stable neutrinos. The green dashed curve is for the case when  $\nu_3$  is taken as unstable with  $\tau_3/m_3 = 1.2 \times 10^{-11}$  s/eV in the data, but in the fit we keep it to be stable. Decay in the data is seen to bring nearly no change to the CP-violation

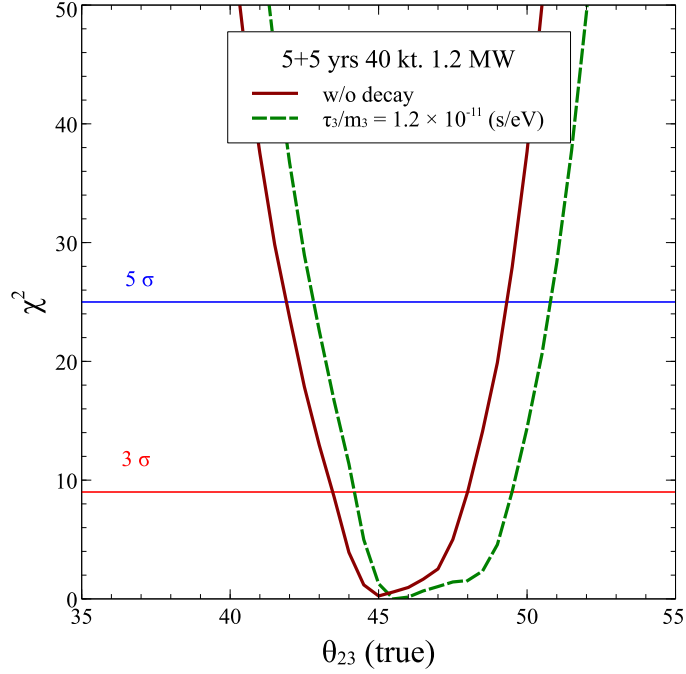


FIG. 7: Expected octant sensitivity at DUNE. The dark red solid curve is for standard case of stable neutrinos. The green dashed curve is for the case when  $\nu_3$  is taken as unstable with  $\tau_3/m_3 = 1.2 \times 10^{-11}$  s/eV in the data, but in the fit we keep it to be stable.

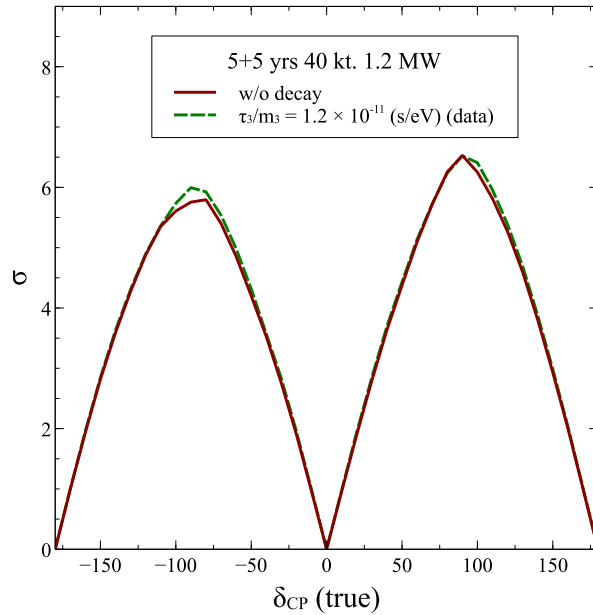


FIG. 8: Expected CP-violation sensitivity at DUNE. The dark red solid curve is for standard case of stable neutrinos. The green dashed curve is for the case when  $\nu_3$  is taken as unstable with  $\tau_3/m_3 = 1.2 \times 10^{-11}$  s/eV in the data, but in the fit we keep it to be stable.

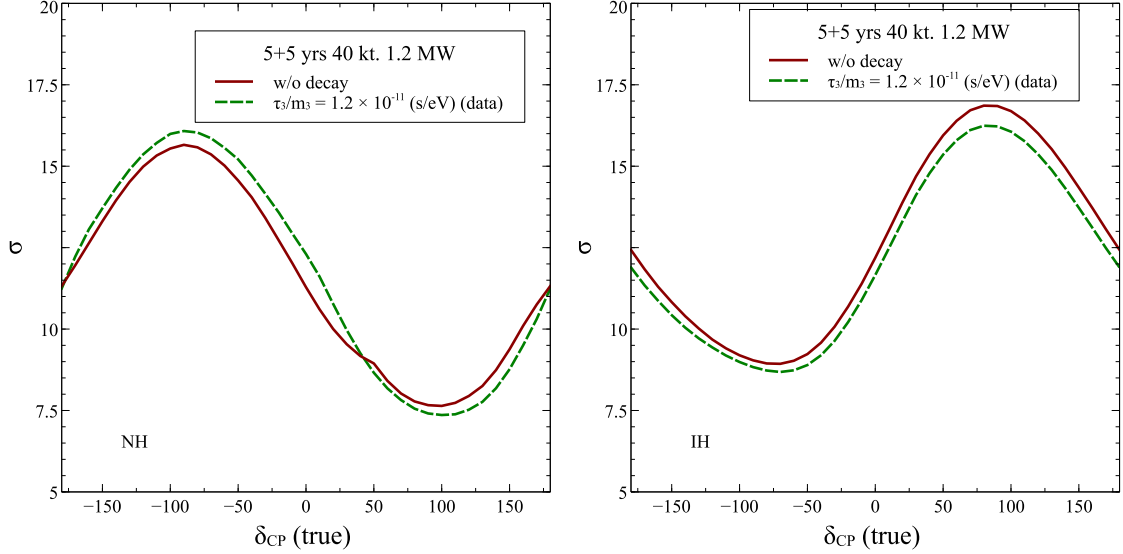


FIG. 9: Expected mass hierarchy sensitivity at DUNE. The dark red solid curve is for standard case of stable neutrinos. The green dashed curve is for the case when  $\nu_3$  is taken as unstable with  $\tau_3/m_3 = 1.2 \times 10^{-11}$  s/eV in the data, but in the fit we keep it to be stable. The left-panel is for NH true while the right-panel is for IH true.

sensitivity of DUNE, with only a marginal increase in the CP-violation sensitivity seen at  $\delta_{CP}(\text{true}) \simeq \pm 90^\circ$ .

The impact of decay on the expected mass hierarchy sensitivity at DUNE is shown in Fig. 9 for both normal hierarchy (NH) true (left-panel) and inverted hierarchy (IH) true (right-panel). As in all figures shown so-far, the dark red solid curve is for standard case of stable neutrinos. The green dashed curve is for the case when  $\nu_3$  is taken as unstable with  $\tau_3/m_3 = 1.2 \times 10^{-11}$  s/eV in the data, but in the fit we keep it to be stable. For IH true, the effect of decay in data is to marginally reduce the expected mass hierarchy sensitivity for all values of  $\delta_{CP}(\text{true})$ . The impact for the NH true case is more complicated with the expected sensitivity increasing for some values of  $\delta_{CP}(\text{true})$  and decreasing for others. However, the net change in the expected sensitivity is seen to be very small compared to the expected mass hierarchy sensitivity at DUNE. Therefore, we conclude that the expected CP-violation sensitivity and mass hierarchy sensitivity at DUNE remain largely unmodified, whether or not neutrinos decay.

## V. SUMMARY & CONCLUSION

We have studied the impact of invisible neutrino decay for the DUNE experiment. We assume the third mass eigenstate is unstable and decays to a very light sterile neutrino. The mass of this state  $m_4$  is assumed to be smaller than the mass of the third mass eigenstate  $m_3$  irrespective of the hierarchy. We do a full three generation study incorporating the matter effects in our numerical simulations. First, we have studied the sensitivity of DUNE to constrain the parameter  $\tau_3/m_3$  and obtained the bound  $\tau_3/m_3 > 4.50 \times 10^{-11}$  s/eV at 90% C.L. for NH, 5+5 year of DUNE data and a 40 kt detector volume. This is one order of magnitude improvement over the bound obtained in [35] from combined MINOS and T2K data. We also studied the potential of DUNE to discover neutrino decay, should it exists in nature and found that DUNE can discover a decaying neutrino scenario for  $\tau_3/m_3 > 4.27 \times 10^{-11}$  s/eV at 90% C.L. with its projected run. In addition, we explored how precisely DUNE can constrain the decay parameter and showed that for an unstable  $\nu_3$  with  $\tau_3/m_3 = 1.2 \times 10^{-11}$  s/eV, the no decay case gets excluded at  $3\sigma$ . At 90% C.L. the allowed range corresponding to this true value is given as  $1.71 \times 10^{-11} > \tau_3/m_3 > 9.29 \times 10^{-12}$  in units of s/eV.

We showed that an interesting correlation exists between the decay life time and the parameter  $\theta_{23}$  in the appearance probability  $P_{\mu e}$ . For values of  $\tau_3/m_3$  for which fast invisible decay relevant for the baseline under consideration occurs the probability  $P_{\mu e}$  decreases. This decrease can be compensated by a higher value of  $\sin^2 \theta_{23}$ . Alternatively, if we assume decay to be present in the data then it can be mimicked by a no decay scenario for a lower value of  $\theta_{23}$  leading to an erroneous determination of the latter. Since it is well known that determination of  $\theta_{23}$  is correlated with the value of  $\theta_{13}$ , we presented contours in the  $\theta_{23} - \theta_{13}$  plane assuming decay in data and fitting it with a model with no decay. We found that the contours show a trend to move towards lower  $\theta_{23}$  value. The allowed range of  $\theta_{13}$  also spreads as compared to the only oscillation case, but the effect is more drastic for  $\theta_{23}$ . We did not observe this kind of correlation between  $\tau_3/m_3$  and  $\theta_{23}$  for the  $P_{\mu\mu}$  channel and hence a combination of the disappearance and appearance data can break the  $\tau_3/m_3 - \theta_{23}$  degeneracy. We also studied the impact of a decaying neutrino on the determination of hierarchy, octant and  $\delta_{CP}$  at DUNE. For this we generated the data assuming decay and fitted it with a theory with no-decay. The maximum effect was seen to be on the octant determination for which

for true  $\theta_{23}$  in the lower octant (higher octant) the octant discrimination capability increases (decreases). The invisible decay scenario considered in this work affects the hierarchy and CP sensitivity of DUNE nominally. In conclusion, the DUNE experiment provides an interesting testing ground for the invisible neutrino decay hypothesis for  $\tau_3/m_3 \sim 10^{-11}$  s/eV.

Note Added : While we were finalizing this work, ref. [15] came, which also addresses exploration of neutrino decay at DUNE. Their emphasis is more on visible decay though they also provide a comparison with the invisible decay case. We consider invisible decays to light sterile neutrinos and have explored different parameter spaces. Hence the two works supplement each other. We also discussed the impact of decay on the determination of  $\theta_{23}$  and its octant. In addition we also studied the effect of decay on mass hierarchy and  $\delta_{CP}$  discovery at DUNE.

### Acknowledgment

We acknowledge the HRI cluster computing facility (<http://cluster.hri.res.in>). SG would like to thank Lakshmi. S. Mohan, Chandan Gupta and Subhendra Mohanty for discussions. This project has received funding from the European Union's Horizon 2020 research and innovation programme InvisiblesPlus RISE under the Marie Skłodowska-Curie grant agreement No 690575. This project has received funding from the European Union's Horizon 2020 research and innovation programme Elusives ITN under the Marie Skłodowska-Curie grant agreement No 674896.

- 
- [1] F. Capozzi, E. Lisi, A. Marrone, D. Montanino, and A. Palazzo, Nucl. Phys. **B908**, 218 (2016), 1601.07777.
  - [2] I. Esteban, M. C. Gonzalez-Garcia, M. Maltoni, I. Martinez-Soler, and T. Schwetz, JHEP **01**, 087 (2017), 1611.01514.
  - [3] K. Abe et al. (T2K), Phys. Rev. Lett. **118**, 151801 (2017), 1701.00432.
  - [4] P. Adamson et al. (NOvA), Phys. Rev. Lett. **116**, 151806 (2016), 1601.05022.
  - [5] P. Adamson et al. (NOvA) (2017), 1703.03328.
  - [6] S. Goswami and N. Nath (2017), 1705.01274.
  - [7] A. Acker, S. Pakvasa, and J. T. Pantaleone, Phys. Rev. **D45**, 1 (1992).

- [8] A. Acker and S. Pakvasa, Phys. Lett. **B320**, 320 (1994), hep-ph/9310207.
- [9] G. B. Gelmini and M. Roncadelli, Phys. Lett. **99B**, 411 (1981).
- [10] Y. Chikashige, R. N. Mohapatra, and R. D. Peccei, Phys. Lett. **B98**, 265 (1981).
- [11] S. Pakvasa, AIP Conf. Proc. **542**, 99 (2000), [,99(1999)], hep-ph/0004077.
- [12] C. W. Kim and W. P. Lam, Mod. Phys. Lett. **A5**, 297 (1990).
- [13] A. Acker, A. Joshipura, and S. Pakvasa, Phys. Lett. **B285**, 371 (1992).
- [14] M. Lindner, T. Ohlsson, and W. Winter, Nucl. Phys. **B607**, 326 (2001), hep-ph/0103170.
- [15] P. Coloma and O. L. G. Peres (2017), 1705.03599.
- [16] A. M. Gago, R. A. Gomes, A. L. G. Gomes, J. Jones-Perez, and O. L. G. Peres (2017), 1705.03074.
- [17] J. N. Bahcall, N. Cabibbo, and A. Yahil, Phys. Rev. Lett. **28**, 316 (1972).
- [18] Z. G. Berezhiani, G. Fiorentini, M. Moretti, and A. Rossi, Z. Phys. **C54**, 581 (1992).
- [19] Z. G. Berezhiani, M. Moretti, and A. Rossi, Z. Phys. **C58**, 423 (1993).
- [20] S. Choubey, S. Goswami, and D. Majumdar, Phys. Lett. **B484**, 73 (2000), hep-ph/0004193.
- [21] A. Bandyopadhyay, S. Choubey, and S. Goswami, Phys. Rev. **D63**, 113019 (2001), hep-ph/0101273.
- [22] A. S. Joshipura, E. Masso, and S. Mohanty, Phys. Rev. **D66**, 113008 (2002), hep-ph/0203181.
- [23] A. Bandyopadhyay, S. Choubey, and S. Goswami, Phys. Lett. **B555**, 33 (2003), hep-ph/0204173.
- [24] R. Picoreti, M. M. Guzzo, P. C. de Holanda, and O. L. G. Peres, Phys. Lett. **B761**, 70 (2016), 1506.08158.
- [25] J. M. Berryman, A. de Gouvea, and D. Hernandez, Phys. Rev. **D92**, 073003 (2015), 1411.0308.
- [26] J. A. Frieman, H. E. Haber, and K. Freese, Phys. Lett. **B200**, 115 (1988).
- [27] J. M. LoSecco (1998), hep-ph/9809499.
- [28] V. D. Barger, J. G. Learned, S. Pakvasa, and T. J. Weiler, Phys. Rev. Lett. **82**, 2640 (1999), astro-ph/9810121.
- [29] P. Lipari and M. Lusignoli, Phys. Rev. **D60**, 013003 (1999), hep-ph/9901350.
- [30] G. L. Fogli, E. Lisi, A. Marrone, and G. Scioscia, Phys. Rev. **D59**, 117303 (1999), hep-ph/9902267.
- [31] S. Choubey and S. Goswami, Astropart. Phys. **14**, 67 (2000), hep-ph/9904257.
- [32] V. D. Barger, J. G. Learned, P. Lipari, M. Lusignoli, S. Pakvasa, and T. J. Weiler, Phys. Lett.

- B462**, 109 (1999), hep-ph/9907421.
- [33] Y. Ashie et al. (Super-Kamiokande), Phys. Rev. Lett. **93**, 101801 (2004), hep-ex/0404034.
- [34] M. C. Gonzalez-Garcia and M. Maltoni, Phys. Lett. **B663**, 405 (2008), 0802.3699.
- [35] R. A. Gomes, A. L. G. Gomes, and O. L. G. Peres, Phys. Lett. **B740**, 345 (2015), 1407.5640.
- [36] T. Abraho, H. Minakata, H. Nunokawa, and A. A. Quiroga, JHEP **11**, 001 (2015), 1506.02314.
- [37] J. F. Beacom, N. F. Bell, D. Hooper, S. Pakvasa, and T. J. Weiler, Phys. Rev. Lett. **90**, 181301 (2003), hep-ph/0211305.
- [38] M. Maltoni and W. Winter, JHEP **07**, 064 (2008), 0803.2050.
- [39] S. Pakvasa, A. Joshipura, and S. Mohanty, Phys. Rev. Lett. **110**, 171802 (2013), 1209.5630.
- [40] G. Pagliaroli, A. Palladino, F. L. Villante, and F. Vissani, Phys. Rev. **D92**, 113008 (2015), 1506.02624.
- [41] M. Bustamante, J. F. Beacom, and K. Murase, Phys. Rev. **D95**, 063013 (2017), 1610.02096.
- [42] J. M. Berryman, A. de Gouvea, D. Hernandez, and R. L. N. Oliveira, Phys. Lett. **B742**, 74 (2015), 1407.6631.
- [43] A. M. Dziewonski and D. L. Anderson, Phys. Earth and Planet Int. **25**, 297 (1981).
- [44] R. Acciarri et al. (DUNE) (2016), 1601.05471.
- [45] R. Acciarri et al. (DUNE) (2015), 1512.06148.
- [46] J. Strait et al. (DUNE) (2016), 1601.05823.
- [47] R. Acciarri et al. (DUNE) (2016), 1601.02984.
- [48] P. Huber, M. Lindner, and W. Winter, Comput. Phys. Commun. **167**, 195 (2005), hep-ph/0407333.
- [49] P. Huber, J. Kopp, M. Lindner, M. Rolinec, and W. Winter, Comput. Phys. Commun. **177**, 432 (2007), hep-ph/0701187.